Surface-enhanced Raman scattering from copper nanoparticles treated furanoflavonoid karanjin

Prahlad K. Baruah[1], Anuma Singh[2], Iffat Jahan[2], Latha Rangan[2], Aditya N. Panda[3], Ashwini K. Sharma[1], Alika Khare[1]*

[1]*Department of Physics, Indian Institute of Technology Guwahati, Guwahati 781039, India*
[2]*Department of Biosciences and Bioengineering, Indian Institute of Technology Guwahati, Guwahati 781039, India*
[3]*Department of Chemistry, Indian Institute of Technology Guwahati, Guwahati 781039, India*

*Corresponding author. Tel: (+91) 361 258 2705; Email: alika@iitg.ernet.in

Received: 09 January 2017, Revised: 16 February 2017 and Accepted: 09 April 2017

DOI: 10.5185/amlett.2017.1612
www.vbripress.com/aml

Abstract

The effect of concentration of copper (Cu) nanoparticles (NPs) on surface enhanced Raman scattering (SERS) in furanoflavonoid karanjin is reported in this paper. Cu NPs were synthesized by pulsed laser ablation of Cu target immersed in distilled water (DW). The absorption spectrum of colloidal solution of Cu NPs displayed a broad peak around ~625 nm corresponding to the surface plasmon resonance (SPR) oscillations. Transmission electron microscope (TEM) images confirmed the formation of nearly spherical Cu NPs having average size of ~12-13 nm. The solution of furanoflavonoid karanjin dissolved in dimethyl sulphoxide (DMSO) was treated with the synthesized NPs and subjected to micro-Raman spectrophotometer for the SERS studies as a function of concentration of Cu NPs. Raman signal of Cu NP treated karanjin was observed to be ten times more as compared to that of untreated one for the most intense C=O stretching band of flavone ring. This corresponds to an enhancement factor of the order of 10^2 and was observed at the optimum concentration of ~0.08 mg/mL of Cu NPs. Copyright © 2017 VBRI Press.

Keywords: Surface enhanced raman scattering, copper nanoparticles, surface plasmon resonance, furanoflavonoid.

Introduction

Surface enhanced Raman scattering (SERS) is a vibrational spectroscopic technique which can be used to enhance the intensity of intrinsically weak Raman signal from a sample by several orders of magnitude **[1-5]**. Traditional Raman spectroscopy although is very efficient in terms of identification of species, it has an obvious disadvantage of low signal. This is due to the low cross-section for the Raman scattering. But this disadvantage has been negated most notably by the advent of SERS. The virtue of SERS lies in its ability to identify different species and obtain structural information for a wide variety of fields including biomedical engineering, material science, electrochemistry, etc. **[1, 5, 6]**.

The amplification of the signal in SERS can be explained through two main mechanisms. In the first mechanism, the electromagnetic enhancement, light interacts with metal NPs to form plasmons and its energy causes the enhancement of Raman signal of the adsorbed molecule **[1, 5]**. The other main mechanism, the chemical enhancement, is attributed to the charge transfer between the metal and the adsorbed molecule. In almost all cases of SERS effect, metals appear in the form of metallic nanostructures. The mechanism of SERS highly depends on the interaction between the surface of the nanostructures and the adsorbed molecules. Even though, since its discovery, more than 35 years ago, many advances have been made in the search for high-performance SERS substrates but till date the quest for more reliable and low cost SERS substrates is on **[7, 8]**. In an SERS experiment, there are many parameters that can be varied but out of these there are two that stand out viz., the species to be detected and the metallic nanostructures. The former being the probe and the latter is the SERS substrate. The choice of the probe and substrate is crucial and it is to be ensured that there should be a proper interaction between them to profit from the amplification of Raman signals. Coinage metals like gold (Au), silver (Ag), or copper (Cu) are known to exhibit localized surface plasmon resonance bands in the visible region and therefore have been extensively used as SERS substrates **[9-12]**. In terms of applicability, Au and Ag being more stable are popular as compared to Cu which is more reactive. Chemically prepared Au and Ag colloids are reported to drastically enhance the Raman signal of various analytes such as alpha-tocopherol and phenethylamines, having weak Raman signal **[13, 14]**. But the low cost and applicability of Cu NPs as catalyst and in various biochemical applications has motivated many researchers to use Cu as an effective SERS substrate **[15-17]**.

To substantiate this, in the present work, Cu NPs have been synthesized by the very effective and simple method of pulsed laser ablation in liquid (PLAL) **[18]**. Focusing of a high power laser onto the target results in ablation of the material and plasma formation. The surrounding liquid confines the plasma and as a result the plasma achieves a state of high temperature, high pressure and high density regime. These extreme conditions favor the formation of nanoparticles **[18, 19]**. This method for the synthesis of NPs to prepare the SERS substrate is preferred over chemical methods owing to its environment friendly nature as it does not involve any hazardous reagent **[18]**. The capability of the synthesized NPs to produce SERS is desirable for the possibility of sensitive structural detection of analytes having weak Raman signal such as flavonoids and/or of low concentration. Flavonoids are known to exhibit strong antioxidant properties and are also one of the main components of many natural dyes making it very useful in pharmaceutical and textile industries **[20]**. One of such compounds is karanjin (3-methoxy furano-2,3,7,8-flavone), a bioactive furanoflavonoid isolated from the seeds of Pongamia pinnata **[21, 22]**. Keeping in view the importance of the detection of such flavonoids, the prepared Cu NPs have been used to increase the Raman intensity of karanjin through SERS.

Experimental

Materials / chemicals details

For the synthesis of the Cu NPs, a clean Cu target (99.98% pure, metals basis, SIGMA ALDRICH) was placed at the bottom of a glass beaker filled with 8 mL of DW.

Material synthesis / reactions

The 2nd harmonic of a Q-switched Nd:YAG laser (Model: Litron LPY7864-10G) having a pulse duration of 10 ns was used for ablating the target. The laser was operated at a repetition rate of 10 Hz. The laser beam was steered suitably using a set of optical components and then focused by a 25 cm focal length lens onto the target immersed in DW. The target was irradiated for 60 minutes while keeping the laser energy fixed at 40 mJ. To facilitate the availability of fresh area of ablation with each laser shot, the target was continuously translated with the help of a motorized translational stage.

Karanjin was isolated from ethyl acetate crude extract by column chromatography using hexane-ethyl acetate eluent system. The compound was purified and the R_f value of karanjin was found to be 0.44 in 15% hexane-ethyl acetate eluent system. After crystallization, white needle-shaped crystal was obtained. The process of recovery through crystallization was very efficient in achieving a yield of pure karanjin crystals up to approximately 2%. The crystals were washed with hexane and binary solvent mixture (ethyl acetate and hexane). As karanjin is not soluble in water, the prepared karanjin crystals were dissolved in DMSO to obtain a concentration of 2 mg/mL. To check the SERS capability of the synthesized Cu NPs on karanjin, the prepared colloid of Cu NPs having a concentration of ~0.40 mg/mL was diluted by adding DW to make 5 more samples of Cu NPs with concentrations of ~0.32 mg/mL, ~0.24 mg/mL, ~0.16 mg/mL, ~0.08 mg/mL and ~0.04 mg/mL. To 200 µL of each of these six samples of Cu NPs, 10 µL of karanjin was added. The solutions were then sonicated for proper mixing and attachment and then drop cast onto two separate silicon wafers which were cleaned by ultrasonication in acetone.

Characterizations / device fabrications / response measurements

The absorption spectrum of the prepared colloid of Cu NPs in DW was recorded using a UV-Visible spectrophotometer (Model: Shimadzu UV-3101 PC). The dried samples were taken for recording the Raman spectra (Model: Horiba Jobin Yvon, LabRam HR 800) with an excitation wavelength of 488 nm. The size and shape of the nanoparticles as well as the attachment of Cu NPs onto karanjin were investigated by TEM (Model: JEOL JEM-2100). For this, the colloidal solution of Cu NPs and that of Cu NPs mixed with karanjin were drop cast onto two carbon coated 300 mesh copper grids and taken for TEM analysis.

Results and discussion

The absorption spectrum of the colloidal solution of Cu NPs is shown in **Fig. 1**.

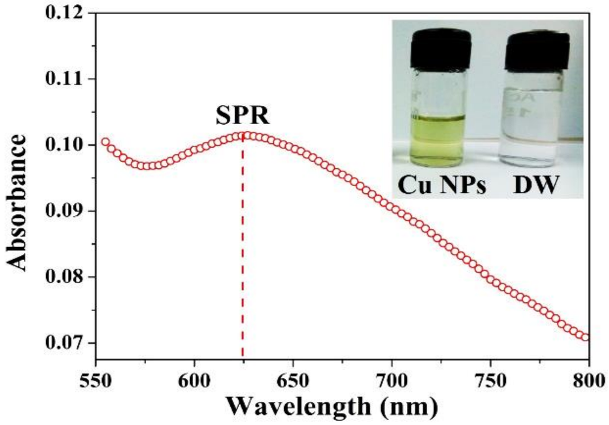

Fig. 1. Absorption spectrum of the prepared colloidal solution of Cu NPs; inset shows change in color of colloidal solution.

The broad absorption peak in the visible region around 625 nm is due to surface plasmon resonance (SPR) in Cu NPs **[23-25]**. The broad peak suggests the formation of small size particles which was later verified by the TEM image. The SPR peak of Cu usually lies in 570-590 nm range **[26]**. The red shift in the SPR peak can be attributed to the formation of both Cu as well as its oxide NPs due to partial oxidation of Cu during ablation **[23, 26]**. The formation of NPs is further confirmed by the appearance of a green color in the prepared colloids as can be seen in the inset of **Fig. 1**.

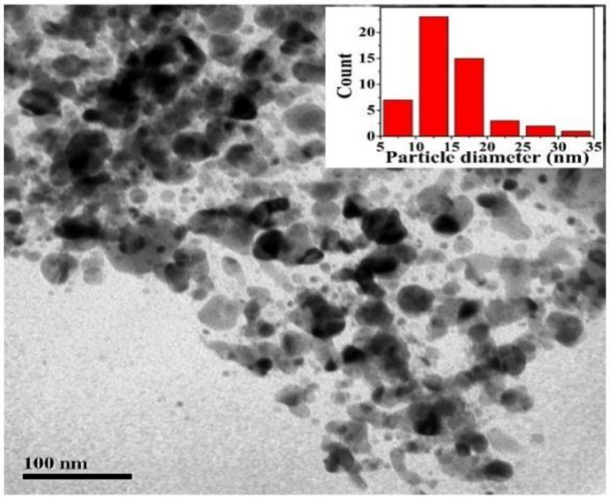

Fig. 2. TEM image of the Cu NPs; inset shows the corresponding particle size distribution of the Cu NPs.

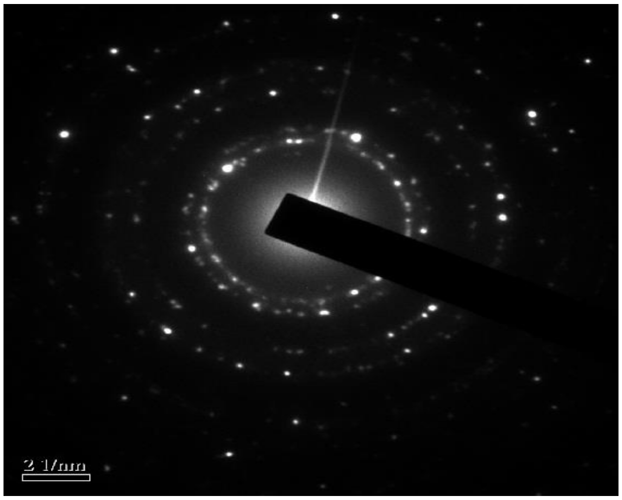

Fig. 3. SAED pattern of the prepared NPs.

Fig. 2 shows the TEM image of the prepared Cu NPs and the corresponding particle size distribution in the inset. The diameter of the NPs is ascertained using the ImageJ software available freely. The average particle size of the NPs is approximately 12-13 nm as can be seen in the distribution. It is to be noted that while determining the particle size, the overlapping particles have been ignored. The selected area electron diffraction (SAED) pattern of the NPs, shown in **Fig. 3**, was used to gain an insight into its structural features. The calculated d-values of 0.29 nm, 0.20 nm, 0.17 nm and 0.13 nm correspond to Cu_2O (110), Cu (111), CuO (020) and Cu_2O (311), respectively. The SPR observation together with SAED pattern indicates the formation of Cu@Cu_xO (x=1, 2).

For the phenomenon of SERS, the NPs should get attached to or be in the vicinity of the analyte. The samples prepared in the present work fulfil this criterion as depicted by the TEM image in **Fig.4**. It clearly shows the Cu NPs attached to the karanjin crystal. The Raman spectrum of untreated karanjin and also of the six samples of karanjin treated with Cu NPs of different concentration were recorded. To validate the results, density functional theory (DFT) calculations were carried out at B3LYP/6-311+G (d, p) level using the Gaussian 09 software **[27]**.

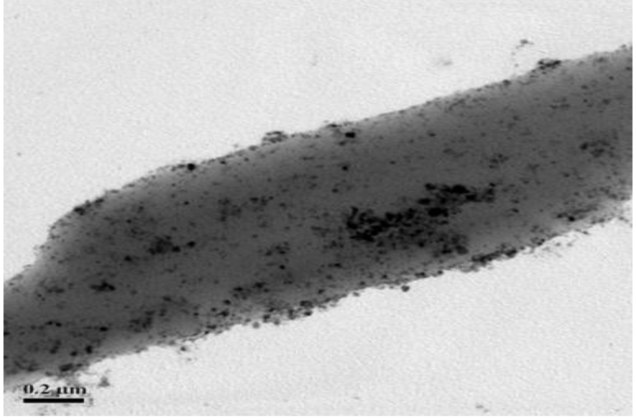

Fig. 4. TEM image of the Cu NPs attached to karanjin.

Table 1. Vibrational assignments of Raman bands of karanjin.

DFT Raman shift (cm^{-1})	**Untreated Karanjin Raman shift (cm^{-1})**	**Karanjin treated with Cu NP (max. SERS) Raman shift (cm^{-1})**	**Assignments**
-	-	1004	Trigonal stretch of flavone B ring
1016	-	1019	CH- vibration in the furan ring
1043	-	-	-
1076	-	-	-
1158	-	1166	-
-	-	1189	Bending of CH-plane
1212	-	-	-
1244	-	-	-
1264	-	-	-
1299	1286	1286	Bending of CH-plane
-	1342	1342	CH- vibration in the furan ring
1363	1368	1372	Presence of CH_3 group
1384	-	-	-
-	1407	1407	-
1424	-	-	-
-	1437	1437	CH- vibration in the furan ring
1465	-	1460	-
1523	1530	1530	Bending of CH-plane
1563	1573	1570	-
-	1587	1587	-
1599	1603	1600	Strong C=O stretching of flavone ring
1640	1627	1627	
1655	-	-	-
1687	-	-	-

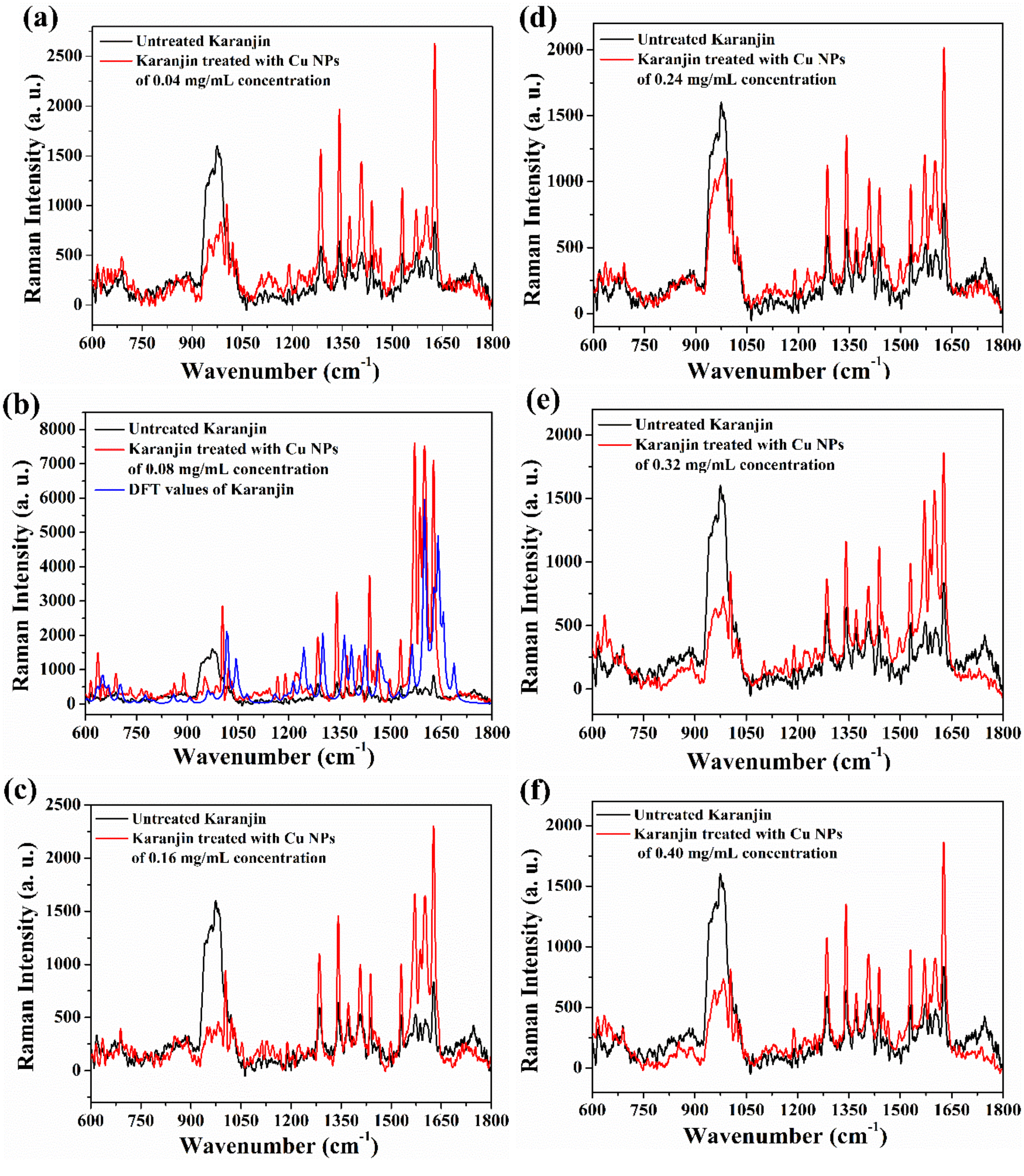

Fig. 5(a)-(f). Raman spectra of untreated karanjin as well as karanjin treated with Cu NPs of different concentrations (**fig. 5(b)** also includes the DFT spectrum of karanjin).

These scaled theoretical wave numbers are in good agreement with the experimental values of pure karanjin crystal as shown in **Fig. 5**. **Table 1** lists the vibrational assignments of some of the Raman bands of karanjin. Here, the Raman shift for karanjin obtained by DFT and experimental values for untreated karanjin and that of karanjin treated with Cu NPs (~0.08 mg/mL concentration corresponding to maximum SERS signal) are listed along with the known vibrational assignments **[22]**. It has been observed that some of the bands which did not appear in the Raman spectrum of untreated karanjin have been detected in the SERS spectrum.

Fig. 5(a)-(f) show the Raman spectra of untreated karanjin and that of karanjin treated with Cu NPs of different concentration. Each experimental plot in **Fig. 5** is averaged over three scans on different areas of the same sample. On comparing the spectra, a sharp increase in signal intensity is observed in the samples containing Cu NPs as compared to that of untreated karanjin. This increase in the Raman signal is attributed to SERS. The enhancement in intensity is due to the excitation of localized surface plasmons of the Cu NPs attached to as well as the NPs in the vicinity of karanjin. Enhancement of the electric field at the interface and the resonance with the surface plasmon absorption band due to the excitation of the conduction electrons localized at the copper surface are responsible for the observed high SERS intensity.

The ten-fold increase in the Raman intensity in **Fig. 5(b)** for a concentration of ~0.08 mg/mL Cu NPs itself attests the fact that the Raman intensity of karanjin has been boosted by the localized surface plasmons of the Cu NPs. Increase in intensity is also observed in the other samples. In order to quantify the power of SERS, the enhancement factor is a very convenient and common yardstick **[28, 29]**. For SERS enhancement factor, the band appearing at approximately 1627 cm^{-1}, due to strong C=O stretching of flavone ring is used as the reference to calculate the enhancement factor **[30]**. This band is selected because its position hasn't changed after treatment with Cu NPs and its intensity is maximum as compared to all other bands for most of the samples in the present study. The following formula for the calculation of the analytical enhancement factor (E) is used **[11, 28, 29]:**

$$E = \frac{I_{SERS} \times C_{SOL}}{I_{SOL} \times C_{SERS}} \qquad (1)$$

where I_{SERS} is the intensity of the band appearing at approximately 1627 cm^{-1} in the SERS spectrum, I_{SOL} is intensity of the same band in the normal Raman spectrum, C_{SERS} is the concentration of karanjin in the colloid and C_{SOL} is the concentration of karanjin in the solution (DMSO).

In this work, maximum enhancement is observed in the sample with Cu NP concentration of ~0.08 mg/mL and this value corresponds to an enhancement factor of ~1.92×10^2. Although the order of magnitude is only 2 but this should not be a major concern as from **Equation 1** it can be seen that the concentration of both the probe as well as the analyte plays a major role in determining the order of magnitude. By changing the concentration of the analyte, this order can be increased. But as the present investigation is mainly aimed at a qualitative analysis, the values of enhancement factor obtained gives a fairly clear picture.

The plot of enhancement factor versus Cu NP concentration is shown in **Fig. 6**. With the increase in concentration of the Cu NPs from ~0.04 mg/mL to ~0.08 mg/mL, the enhancement factor, E increases and reaches a maximum value. This may be due to increased plasmonic interaction as a result of the presence of more Cu NPs in the vicinity of karanjin. As karanjin is treated with Cu NP samples having higher concentration, the value of E is found to decrease drastically and is almost found to be constant at still higher values of Cu NP concentration. The decrease in the value of E with further increase in concentration may be explained on the basis that due to aggregation of the NPs at higher concentrations the analyte, karanjin is almost completely covered leading to a decrease in signal from the analyte itself. The absorption of light by the plasmon resonance of suspended NPs affects both the incident and the scattered Raman emission **[29]**. This trend of increase followed by a decrease in the value of E is an interesting observation and hints at a definite NP concentration dependence of the SERS enhancement. Although an enhancement in the Raman signal is observed in all the samples, the enhancement in the sample with ~0.08 mg/mL concentration of Cu NPs is quite significant with a ten-fold increase in signal. This concentration is the optimum concentration for the prepared Cu NPs. Thus, in the present work, emphasis has been laid on how just by simply adding the optimized concentration of NPs to the analyte the process can be easily applied to detect analytes having intrinsically low Raman signal.

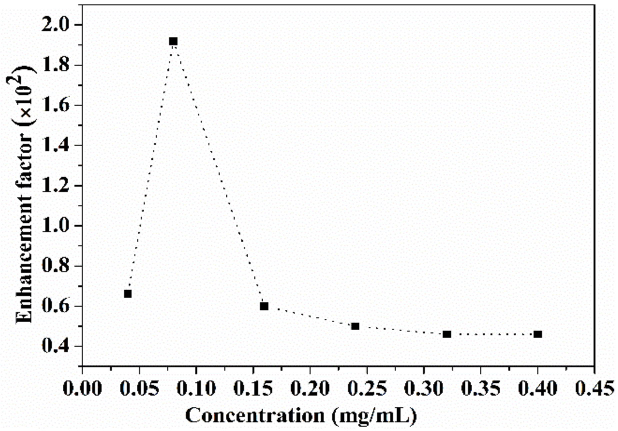

Fig. 6. Variation of enhancement factor with concentration of Cu NPs.

Conclusion

Cu NPs of average particle size ~12-13 nm has been synthesized by the simple method of pulsed laser ablation of Cu in DW. The SAED pattern obtained from TEM confirms the formation of Cu@Cu_xO (x=1, 2) NPs. The appearance of SPR peak in the absorption spectra at ~625 nm further confirmed the formation of Cu NPs. The NPs were mixed with the analyte, a furanoflavonoid, karanjin to demonstrate the enhanced Raman intensity through SERS. The effect of the concentration of Cu NPs on the SERS enhancement factor has been attempted. The optimum concentration of Cu NPs yielding to ten-fold increase in the Raman signal of karanjin was found to be ~0.08 mg/mL.

Acknowledgements

The authors acknowledge the Central Instruments Facility (CIF), IIT Guwahati for the micro-Raman and TEM facility. This work is partially supported by Department of Science and Technology (India), Project No. SR/S2/HEP-18/2009.

Author's contributions

Authors have no competing financial interests.

References

1. Sharma, B; Frontiera, R.R.; Henry, A-I.; Ringe, E.; Van Duyne, R.P.; *Mater. Today*., **2012**, *15(1-2)*, 16.
DOI: 10.1016/S1369-7021(12)70017-2
2. Schlücker, S.; *Angew. Chem. Int. Ed*., **2014**, *53(19)*, 4756.
DOI : 10.1002/anie.201205748
3. Stiles, P. L.; Dieringer, J. A.; Shah, N. C.; Van Duyne, R. P.; *Annu. Rev. Anal. Chem*., **2008**, *1*, 601.
DOI: 10.1146/annurev.anchem.1.031207.112814
4. Moskovits, M.; *J. Raman Spectrosc*., **2005**, *36(6-7)*, 485.
DOI: 10.1002/jrs.1362
5. McNay, G.; Eustace, D.; Smith, W. E.; Faulds, K.; Graham, D.; *Appl. Spectrosc*., **2011**, *65(8)*, 825.
DOI: 10.1366/11-06365
6. Yuen, C.; Zheng, W.; Huang, Z.; *J. Innov. Opt. Heal. Sci*., **2008**, *1(2)*, 267.
DOI: 10.1142/S179354580800025X
7. Sharma, B.; Cardinal, M. F.; Kleinman, S. L.; Greeneltch, N. G.; Frontiera, R. R.; Blaber, M. G.; Schatz, G. C.; Van Duyne, R. P.; *MRS bull*., **2013**, *38*, 615.
DOI: 10.1557/mrs.2013.161
8. Gómez, M.; Lazzari, M.; *Mater. Today*., **2014**, *17(7)*, 358.
DOI: 10.1016/j.mattod.2014.08.001
9. Nguyen, T. B.; Vu, T. K. T.; Nguyen, Q. D.; Nguyen, T. D.; Trinh, T. H.; *Adv. Nat. Sci.: Nanosci. Nanotechnol.*, **2012**, *3*, 025016(1-5).
DOI:10.1088/2043-6262/3/2/025016
10. Herrera, G. M.; Padilla, A. C.; Hernandez-Rivera, S. P.; *Nanomaterials*., **2013**, *3*, 158.
DOI:10.3390/nano3010158
11. Dendisová-Vyškovská, M.; Prokopec, V.; Člupek, M.; Matějka, P.; *J. Raman Spectrosc*., **2012**, *43*, 181.
DOI: 10.1002/jrs.3022
12. Vinod, M.; Gopchandran, K.; *Prog. Nat. Sci. Mater. Int*., **2014**, *24*, 569.
DOI: 10.1016/j.pnsc.2014.10.003
13. Cai, T.; Gu, H.; Liu, F.; Xie, M.; *Appl. Spectrosc.* **2012**, *66(1)*, 114.
DOI: 10.1366/11-06423
14. Taplin, F.; O'Donnell, D.; Kubic, T.; Leona, M.; Lombardi, J.; *Appl. Spectrosc*., **2013**, *67(10)*, 1150.
DOI: 10.1366/13-06990
15. Wang, Y.; Asefa, T.; *Langmuir*, **2010**, *26(10)*, 7469.
DOI:10.1021/la904199f
16. Muniz-Miranda, M.; Gellini, C.; Giorgetti, E.; *J. Phys. Chem. C*., **2011**, *115*, 5021.
DOI: 10.1021/jp1086027
17. Santos, E. d B.; Sigoli, F. A.; Mazali, I. O.; *Mater. Lett.* **2013**, *108*, 172.
DOI: 10.1016/j.matlet.2013.06.110
18. Yang, G.; *Prog. Mater. Sci*., **2007**, *52*, 648.
DOI:10.1016/j.pmatsci.2006.10.016
19. Yan, Z.; Chrisey, D. B.; *J. Photoch. Photobio. C*., **2012**, *13*, 204.
DOI: 10.1016/j.jphotochemrev.2012.04.004
20. Corredor, C.; Teslova, T.; Cañamares, M. V.; Chen, Z.; Zhang, J.; Lombardi, J. R.; Leona, M.; *Vib. Spectrosc*., **2009**, *49*, 190.
DOI:10.1016/j.vibspec.2008.07.012
21. Pandey, A. K.; Bajpai, A. K.; Kumar, A.; Pal, M.; Baboo, V.; Dwivedi, A.; *J. Theor. Chem*., **2014**, *2014*, 1.
DOI: 10.1155/2014/680987
22. Singh, A.; Jahan, I.; Sharma, M.; Rangan, L.; Khare, A.; Panda, A. N.; *Planta Med. Lett*., **2016**.
DOI: 10.1055/s-0042-105159
23. Nath, A.; Khare, A.; *J. Appl. Phys.*, **2011**, *110*, 043111.
DOI: 10.1063/1.3626463
24. Chan, G. H.; Zhao, J.; Hicks, E. M.; Schatz, G. C.; Duyne, R. P. V.; *Nano Lett*., **2007**, *7(7)*, 1947.
DOI: 10.1021/nl070648a
25. Swarnkar, R.; Singh, S.; Gopal, R.; *Bull. Mater. Sci*., **2011**, *34(7)*, 1363.
DOI: 10.1007/s12034-011-0329-4
26. Kazakevich, P.; Simakin, A.; Voronov, V.; Shafeev, G. A.; *Appl. Surf. Sci*., **2006**, *252*, 4373.
DOI: 10.1016/j.apsusc.2005.06.059
27. Frisch, M. J.; et al; *Gaussian 09, Revision D.01. Wallingford, CT: Gaussian, Inc*., **2009**.
28. Ru, E. C. L.; Blackie, E.; Meyer, M.; Etchegoin, P. G.; *J. Phys. Chem. C*., **2007**, *111*, 13794.
DOI: 10.1021/jp0687908
29. Canamares, M. V.; Garcia-Ramos, J.; Sanchez-Cortes, S.; Castillejo, M.; Oujja, M.; *J. Colloid Interf. Sci*., **2008**, *326*, 103.
DOI: 10.1016/j.jcis.2008.06.052
30. Cañamares, M. V.; Lombardi, J. R.; Leona, M.; *e-PS*., **2008**, 81.